J. Mol. Model. **1998**, *4*, 239 – 249

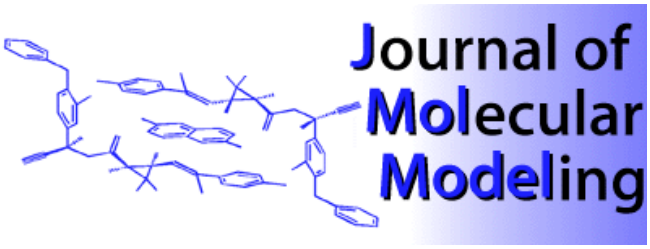

FULL PAPER

From Tumor Necrosis Factor Receptor to RANK, from the Selectins and Link Proteins to CD44: New Molecular Models of Cell Surface Receptors and Analysis of Specificity Determinants

Jürgen Bajorath[1,2]

[1]MDS Panlabs, Computational Chemistry & Informatics, 11804 North Creek Pkwy. S., Bothell, WA, 98011-8805, USA. Tel (425) 487-8297, Fax (425) 487-8262. E-mail: jbajorath@panlabs.com

[2]Department of Biological Structure, University of Washington, Seattle, Washington 98195, USA.

Received: 19 May 1998 / Accepted: 10 July 1998 / Published: 20 July 1998

Abstract Modeling and structure-function studies on two cell surface proteins are presented, which are implicated in the regulation of immune responses and cell adhesion. In the first part, model building of RANK, a new member of the tumor necrosis factor receptor (TNFR) superfamily (TNFRSF), is reported. The model is analyzed in light of structural studies on the TNFR-ligand complex and molecular model-based mutagenesis analyses of CD40-ligand and Fas-ligand interactions. The study makes it possible to predict residues important for ligand binding to RANK and further rationalizes differences in specificity between TNFR-like cell surface receptors. In the second part, recent investigations on the structure and carbohydrate binding site of CD44, a member of the link protein family, are discussed. The binding site in CD44 is compared to calcium-dependent (C-type) lectins, which include the selectins, another family of cell adhesion molecules. The studies on TNFRSF members and link proteins reported herein complement a recent review article in this journal, which focused on modeling and binding site analysis of immune cell surface proteins.

Keywords Cell surface proteins, Protein superfamilies, Molecular models, Binding sites, Specificity

Introduction

The tumor necrosis factor receptor (TNFR) superfamily (TNFRSF) includes many cell surface receptors with important functions in the regulation of immune responses [1]. In addition to TNFR, intensely studied examples include CD40, a receptor critical for B-cell activation and antibody isotype switching [2], Fas (CD95), which controls immune responses by triggering programmed cell death (apoptosis) [3], and 4-1BB (CDw137), which is implicated in T-cell activation [4]. Recently, a new member of the TNFRSF, termed RANK (Receptor Activator of NF-κB), was identified, a type I transmembrane protein with an extracellular TNFR-homologous region [5]. RANK is expressed on dendritic cells, which are major antigen-presenting cells in the immune system with a critical role in lymphocyte activation and the induction of T-cell tolerance to self-antigens [6]. The identification of RANK and its ligand on T-cells

Correspondence to: J. Bajorath, MDS Panlabs

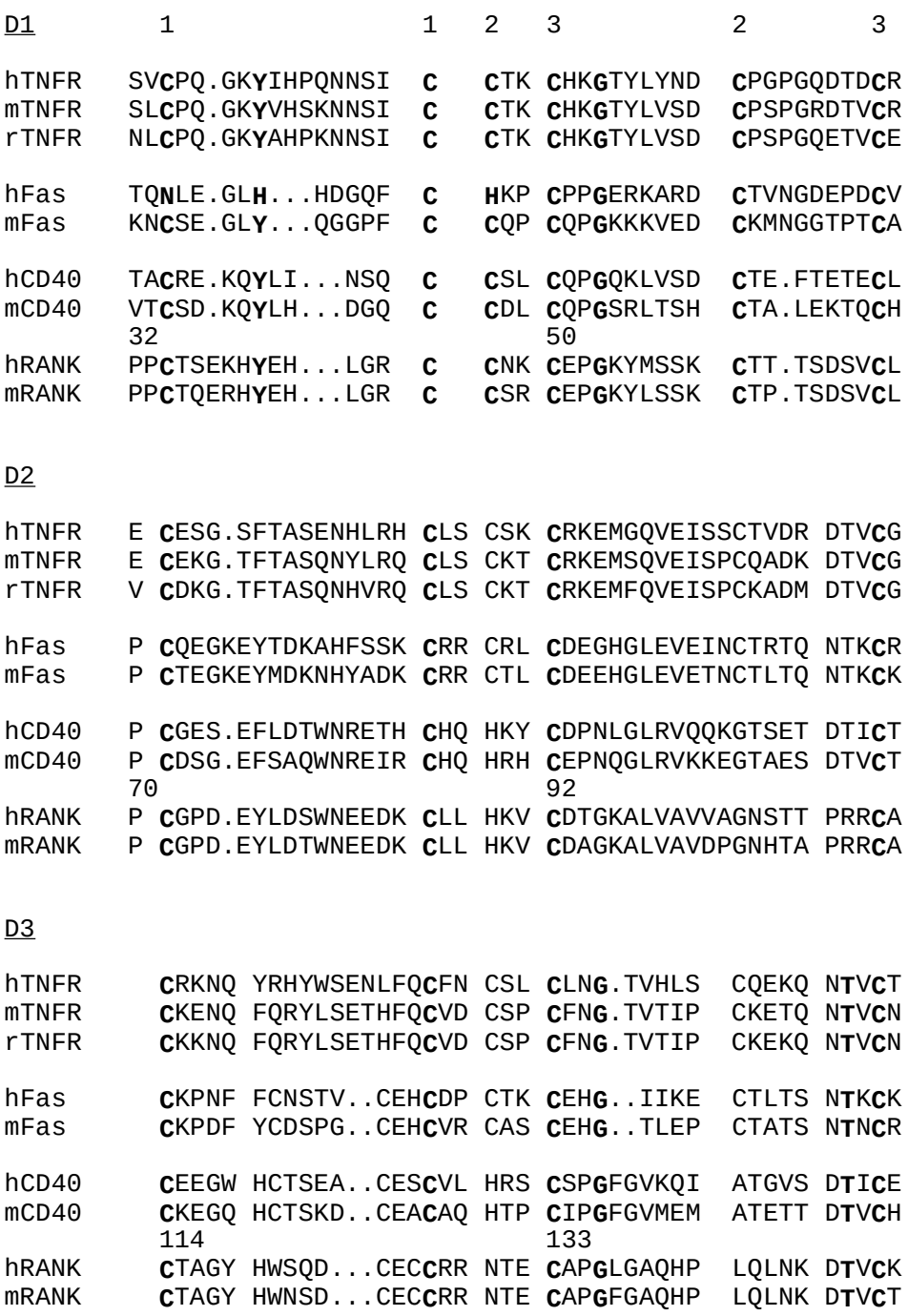

Figure 1 Alignment of extracellular region sequences of TNFR, Fas, CD40, and RANK. *Sequences of repeat domains (D1, D2, D3) from different species (h: human, m: mouse, r: rat) were aligned with respect to conserved cysteine patterns, a characteristic feature of TNFR-like proteins. The positions of cysteine residues forming three canonical disulfide bonds are labeled (1, 2, 3). Spaces are introduced to align corresponding canonical cysteine positions in all domains. Dots indicate deletions. Residues which are identical in at least eight of nine sequences are shown in bold face. Residue numbers are given for RANK*

[5] provides an opportunity to study the interaction between dendritic cells and T-cells at the molecular level and to investigate dendritic cell signaling events. Signaling through RANK is thought to greatly contribute to dendritic cell-dependent T-cell priming and expansion [5], and RANK is therefore of significant interest to molecular immunologists.

TNFRSF proteins share a characteristic extracellular cysteine-rich repeat domain structure [7]. TNFR repeat domains typically include 40-50 residues and display conserved cysteine motifs and other consensus residues of structural importance [7]. The number of extracellular TNFR repeat domains varies across the TNFRSF, and sequence identities range from ~20% to ~40%. The conserved features of TNFR domains make TNFRSF proteins suitable targets for comparative modeling [8,9]. Combined molecular modeling and mutagenesis studies have been carried out to outline the ligand binding sites in CD40 [10,11] and Fas [12-14], and to compare these proteins to TNFR [14]. On the basis of these studies, non-conserved residues in largely corresponding regions determine ligand binding to these receptor and their

specificity. A molecular model of RANK has been generated to predict the RANK ligand binding site and analyze critical residue positions and their molecular environment. Several residues were identified which are unique to RANK and likely determinants of its specificity.

CD44 is a widely distributed cell surface receptor for hyaluronan (HA) [15], and CD44-HA interactions mediate a variety of adhesive interactions important for cell matrix assembly, tissue development, and immune cell adhesion [16]. CD44 binds HA with its N-terminal domain, which is homologous to cartilage link proteins [15,17]. Based on TSG-6, the first structure of a link protein determined [18], the ligand binding domain of CD44 was modeled [19] and the HA binding site identified by model-based mutagenesis [19]. Link modules display, in part, unexpected structural similarity to calcium-dependent (C-type) lectins [18,20], which include the selectins, another family of cell adhesion molecules [21]. Selectins also bind carbohydrate structures and play a critical role in mediating leukocyte-endothelium interactions during an inflammatory reaction [21,22]. Comparison of CD44 with the C-type lectin domains of the mannose-binding protein (MBP) [23] and E-selectin (ESL) [24], provides insights into calcium-dependent and -independent modes of carbohydrate binding and allows to draw conclusions regarding the evolution of these carbohydrate recognition modules.

The modeling and structure-functions studies on RANK and CD44 complement a recent review in this journal [25] which discussed, among other examples, modeling and binding site analysis of TNFRSF members CD40, Fas, and the selectins. Taken together, studies on TNFRSF proteins provide insights as to how these receptors mediate specific protein-protein interactions on the cell surface, while the results obtained for CD44 extend the knowledge of specific cell surface protein-carbohydrate interactions.

Methods

Sequences of human and mouse RANK [5] were aligned relative to a template including TNFR, CD40, and Fas sequences from different species [12], which was generated by focusing on structurally significant TNFR consensus residues [7]. The model of human RANK was built by comparative modeling on the basis of this alignment and using the X-ray structure of ligand-bound TNFR [7] as template. Interactive model building was carried out with InsightII (Vers. 97.0, MSI, San Diego). Residue replacements were modeled using rotamer conformations [26] following the original side chain path if possible. The backbone conformations of loops with the same length in TNFR and RANK were retained, and insertions and deletions in loops were modeled manually following a previously described protocol [27]. The model was refined by energy minimization with MOE (Molecular Operating Environment, Vers. 1997.09, Chemical Computing Group, Montreal) using the MOE forcefield (see: Labute, P. MOE Forcefield Facilities, on-line article, Chemical Computing Group; http://www.chemcomp.com) and AMBER parameters [28], explicit hydrogen atoms, a distance-dependent dielectric constant 4r, an 8 Å cutoff distance for non-bonded interactions, and initial all-atom constraints of 15 kcal/mol/Å^2. Unconstrained conjugate gradients energy minimization was carried out until the root mean square (rms) derivative of the energy function was ~3 kcal/mol/Å. At this stage, the backbone and non-hydrogen atom rms deviations resulting from minimization were ~0.4 Å and ~0.6 Å, respectively. Alpha carbon rms deviations for pairwise superposition of TNFR and molecular models of CD40 [10], Fas [12], and RANK, including all loops, were less than 2 Å in each case. Stereo-

Figure 2 RANK molecular model. *Residues in TNFR-like repeat domains 1, 2, and 3 are shown in cyan, light blue, and dark blue, respectively. Disulfide bonds are colored gold. Other residues thought to be important for the integrity of the TNFR fold and the structure of RANK are colored magenta*

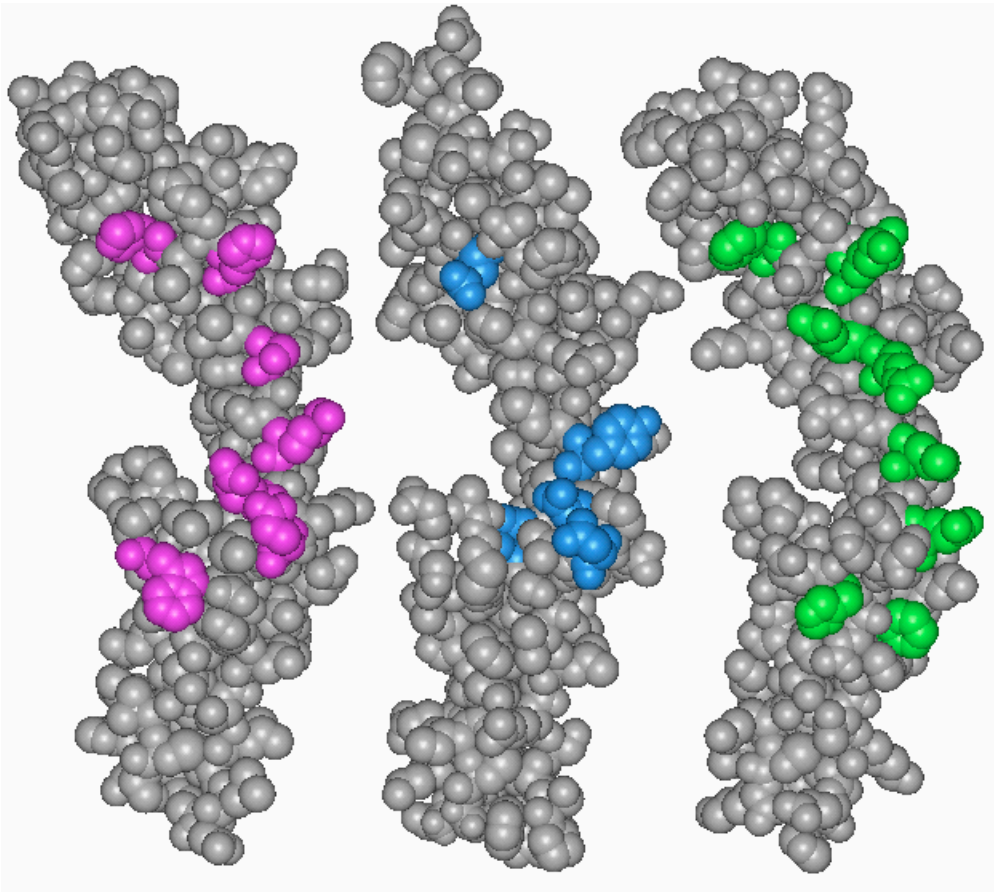

Figure 3a Mapping of residues important for ligand binding. *Residues in TNFR (magenta), CD40 (blue), and Fas (green) are shown which are, on the basis of X-ray (TNFR-ligand complex) or model-based mutagenesis (CD40, Fas) studies, intimately involved in binding*

chemical and intramolecular contact analysis of the RANK model were performed using the protein analysis tools of MOE, and structures were compared using the MOE sequence-structure alignment routines. Computer graphical representations were generated with InsightII. Details concerning the model building procedures and experimental analysis of CD44 are provided in the original publication [19].

Results and discussion

Sequence analysis

The sequence of RANK was compared to TNFR, for which X-ray structures have been reported [7,29], CD40, and Fas. Members of protein superfamilies are evolutionary related and share a basic fold which is, at the sequence level, reflected by the presence of local signature sequence motifs [30]. Since protein superfamiliy members share only low sequence identity, the generation of overall correct sequence alignments by matching local sequence motifs is often problematic [25]. However, RANK could be readily aligned with TNFRSF sequences considering the positions of canonical cysteines and other signature residues. Figure 1 shows the alignment of the extracellular TNFR-like domains, on which the modeling was based. In addition to conserved cysteines, which determine the elongated structure of the TNFR fold by forming a ladder-like arrangement [7], RANK displays other hallmark residues of the TNFR fold. These include the aromatic residues at positions 40, 76, and 118, which form part of the core of the repeat domains, and residues involved in important hydrogen bonding interactions (e.g., 148, 149). In the aligned region, sequence identities of RANK compared to TNFR, Fas, and CD40 are approximately 22%, 27%, and 36%, respectively. Thus, at the sequence level, RANK is more closely related to CD40 than TNFR or Fas. Since CD40 is also expressed on dendritic cells and involved in their activation [31], this relation may be functionally significant.

Molecular model of RANK

The structures of the first three repeat domains in TNFR are well conserved [7,29] and consist of conserved fragments or modules [32]. Models of TNFRSF proteins may therefore either be based on repeat domains [10,12] or combinations of smaller modules [32,33] but differences between these approaches are subtle [33]. Ligand binding to TNFR [7], CD40 [11], and Fas [13,14] has been studied in some detail, and these studies have revealed that binding to all three receptors is centered on domain two and also involves parts of domain

three [7,10,12]. Modeling of human RANK primarily targeted these domains and was based on the structure of ligand-bound TNFR [7]. The modeled region, residues 47-152, also includes about half of the N-terminal domain, the corresponding structure of which was well defined in ligand-bound TNFR [7]. TNFR, CD40, and RANK, but not Fas, have a fourth membrane-proximal domain, which differs in TNFR significantly from the preceding domains [32] and which could not be modeled with confidence in CD40 [10] or RANK. Figure 2 shows the molecular model of human RANK and highlights the canonical cysteine patterns and other structurally important residues. In both CD40 and RANK, the second disulfide bond is absent in domains two and three and replaced by residues forming compensatory interactions [10]. The conformation of loop 123-126 in RANK, including a putative additional disulfide bond C124-C126, could not be modeled without significant distortion of the peptide bond geometry at residue E125 and was deleted from the final model. The molecular model includes only regions of high prediction confidence, a prerequisite for reliable applications [34].

Mapping of residues important for binding

The major purpose of RANK modeling was to predict its ligand binding site and to identify candidate residues likely to be critical for binding. This was possible based on the model-based analysis of data obtained for other TNFRSF receptors. Residues which are intimately involved in TNFRSF receptor-ligand interactions have been identified in TNFR based on crystallographic analysis [7] and in CD40 and Fas by model-based mutagenesis [11,13,14]. The most extensive mutagenesis data are currently available for Fas [14]. Mutagenesis results obtained for CD40 [11] were recently confirmed in an independent study [33]. In Figure 3a, important residues were mapped on the TNFR structure and the Fas and CD40 molecular models. These mapping studies allow to understand the spatial arrangement of important residues and thus to outline and compare the ligand binding sites in these receptors. The comparison shows that residues important for binding map to corresponding regions of these TNFRSF receptors. After optimal superposition of the structures the majority of important residues map to spatially equivalent positions (Figure 3b). However, corresponding residues are generally not conserved in these receptors. These findings imply that different residues at corresponding positions determine the binding specificities of TNFRSF receptor-ligand interactions [14].

Putative ligand binding site in RANK

The above analysis provided the basis for the identification of residues in RANK which are likely to determine its specificity. Therefore, the RANK molecular model was included in the superposition, and the positions of residues important for binding to TNFR, CD40, and Fas were mapped on corresponding positions of the RANK model. It follows that these residues delineate the putative ligand binding region of RANK (Figure 4a). Consistent with this idea, a glycosylation site at position 105 in RANK maps to a solvent-exposed asparagine opposite the putative binding site (and would thus not interfere with ligand binding). In the next step, the putative binding surface in the RANK model was screened for residues not conserved in TNFR, CD40, or Fas. Residues unique to RANK were identified at positions 82, 88, 91, 96, and 118. Figure 4a shows that these residues, when mapped on the model, are distributed over the entire binding site region. Four of the five unique residues are located in sequence segments, which, in other TNFRSF receptors, include the majority of residues important for binding,

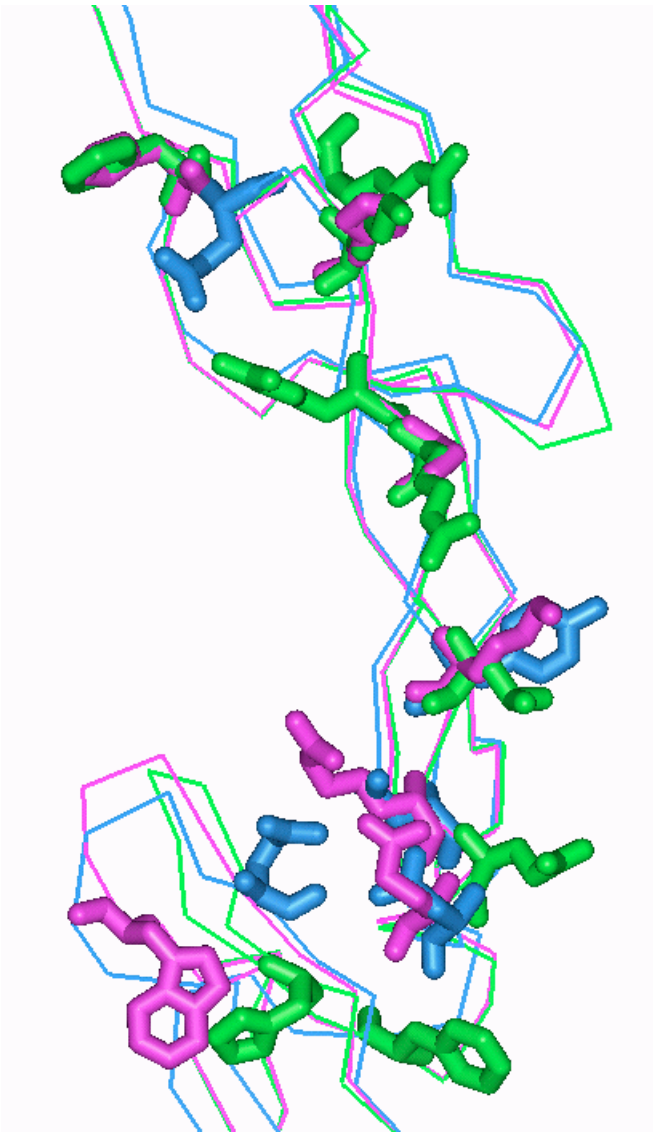

Figure 3b Mapping of residues important for ligand binding. *The residues are shown in a close-up view after optimal superposition of the structures*

and map closely to critical positions (Figure 4b). Two of these residues, E82 and K96, are charged, consistent with the finding that charged residues play an important role in determining TNFRSF receptor-ligand interactions [14,33]. The identified residues are expected to significantly contribute to the specificity of RANK, as they are part of the binding site modeled based on data obtained for homologous receptors but not conserved in these proteins.

Implications and limitations

The modular organization and repeat domain structure of TNFR provides the basis for modeling of other TNFRSF members. Studies on TNFR, CD40, and Fas suggested a common theme for ligand binding to TNFRSF receptors, whereby non-conserved residues at spatially corresponding positions determine the binding of different ligands. The results obtained for RANK are consistent with this paradigm and provide a basis for further experimental structure-function studies. Unlike the immunoglobulin superfamily [35], where many structures are available for comparison [36] and model building [37], modeling of TNFRSF proteins relies on the current structural knowledge of TNFR. Thus, despite significant structural conservation of TNFR modules, additional experimental structures of TNFR-like proteins will help to better understand the association of repeat domains and other structural variations. These insights would further enhance the ability to build molecular models of TNFRSF proteins, as has been the case for C-type lectins where comparison of X-ray structures provided a much improved basis for modeling [38].

CD44, link proteins, and C-type lectins

The cell adhesion molecule CD44 is a variably spliced type I transmembrane protein with diverse functions, which are, in part, isoform-specific [15,16]. CD44 is of considerable interest as a therapeutic target because it can mediate the adhesion and migration of activated leukocytes at sites of inflammation [39] and it is implicated in aggressive tumor metastasis [40]. Adhesion mediated by CD44 usually depends on its interaction with HA, a glycosaminoglycan consisting of a varying number of repeating disaccharide units [41]. The HA binding activity of CD44 resides in its N-terminal domain, which includes ~100 residues and belongs to the link protein family (link module) [16,17]. Link modules are found in extracellular matrix proteins, one of which is the cartilage link protein, and other HA receptor [17]. The C-type lectin family also includes a number of cell surface proteins [20], which, in contrast to link proteins, bind carbohydrate ligands in a calcium-dependent manner [20,23]. Prominent among C-type lectins are the selectins [21], a family of cell adhesion molecules, which recognize Lewis X-type tetrasaccharides [22] and are responsible for the initial interaction between leukocytes and activated vascular endothelium at sites of inflammation [21,22]. Thus, in the immune system, CD44 and the selectins have similar functions [16].

Structural insights

The prototypic C-type lectin fold, as seen in the X-ray structures of MBP [23] and ESL [24], has a high content of irregular secondary structure and includes a conserved calcium binding site, which directly participates in carbohydrate binding [23]. Determination of the first structure of a link module, TSG-6, by NMR [18] revealed rather unexpected similarity with C-type lectin fold [18]. Figure 5 shows a compari-

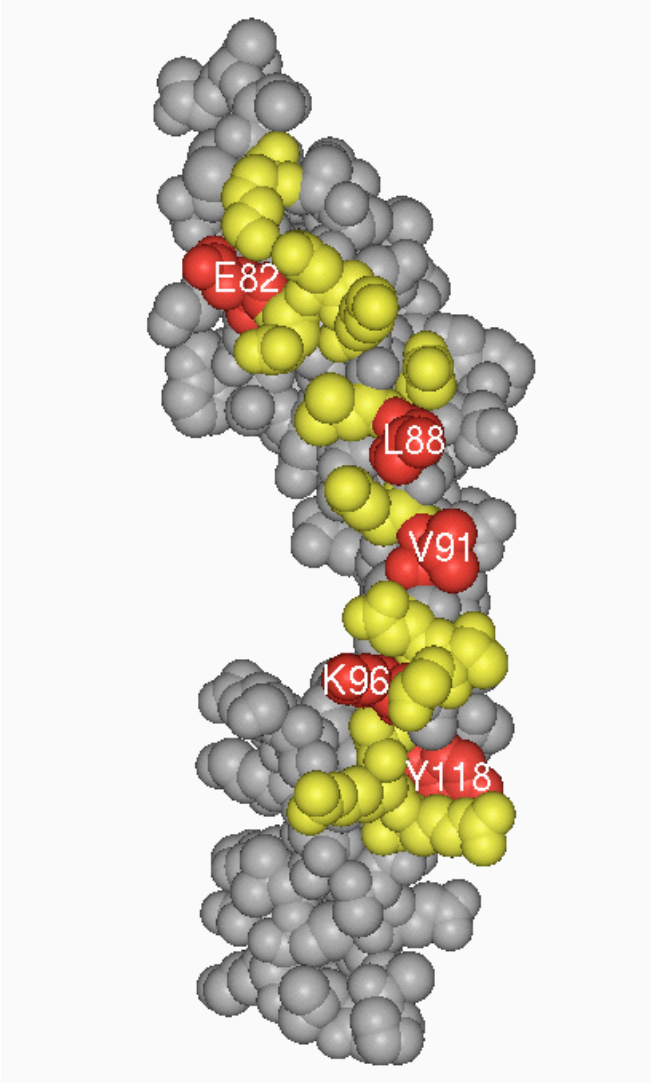

Figure 4a Predicted ligand binding site in RANK. *Residues in RANK which spatially correspond to positions important for ligand binding to TNFR, CD40, and Fas are highlighted in yellow. Residues which are expected to significantly contribute to the specificity of RANK are colored red and labeled*

Figure 4b Predicted ligand binding site in RANK. *Sequence segments including the majority of important residues are shown. The color code is consistent with Figures 3a and 4a*

```
                                66          69          72          75    77    79
hTNFR   A  S  E  N  H  L  R  H  C  L  S  C  S  K  C  R  K  E  M  G
mTNFR   A  S  Q  N  Y  L  R  Q  C  L  S  C  K  T  C  R  K  E  M  S
rTNFR   A  S  Q  N  H  V  R  Q  C  L  S  C  K  T  C  R  K  E  M  F

                             81          84    86 87       90          93
hFas    D  K  A  H  F  S  S  K  C  R  R  C  R  L  C  D  E  G  H  G
mFas    D  K  N  H  Y  A  D  K  C  R  R  C  T  L  C  D  E  E  H  G

                                74                      82    84    86
hCD40   D  T  W  N  R  E  T  H  C  H  Q  H  K  Y  C  D  P  N  L  G
mCD40   A  Q  W  N  R  E  I  R  C  H  Q  H  R  H  C  E  P  N  Q  G

                             82                88          91          96
hRANK   D  S  W  N  E  E  D  K  C  L  L  H  K  V  C  D  T  G  K  A
mRANK   D  T  W  N  E  E  D  K  C  L  L  H  K  V  C  D  A  G  K  A
```

Figure 5 E-selectin, TSG-6, and the CD44 molecular model. *Ribbon representations of ESL (magenta; functional calcium depicted as a sphere), TSG-6 (green), and CD44 (silver). Compared to the orientation of ESL (upper left), the superposition of ESL and TSG-6 (lower left) is shown after rotation of approximately 90° around the vertical axis, while the superposition of TSG-6 and CD44 (lower right) is shown in the same orientation as TSG-6 (upper right)*

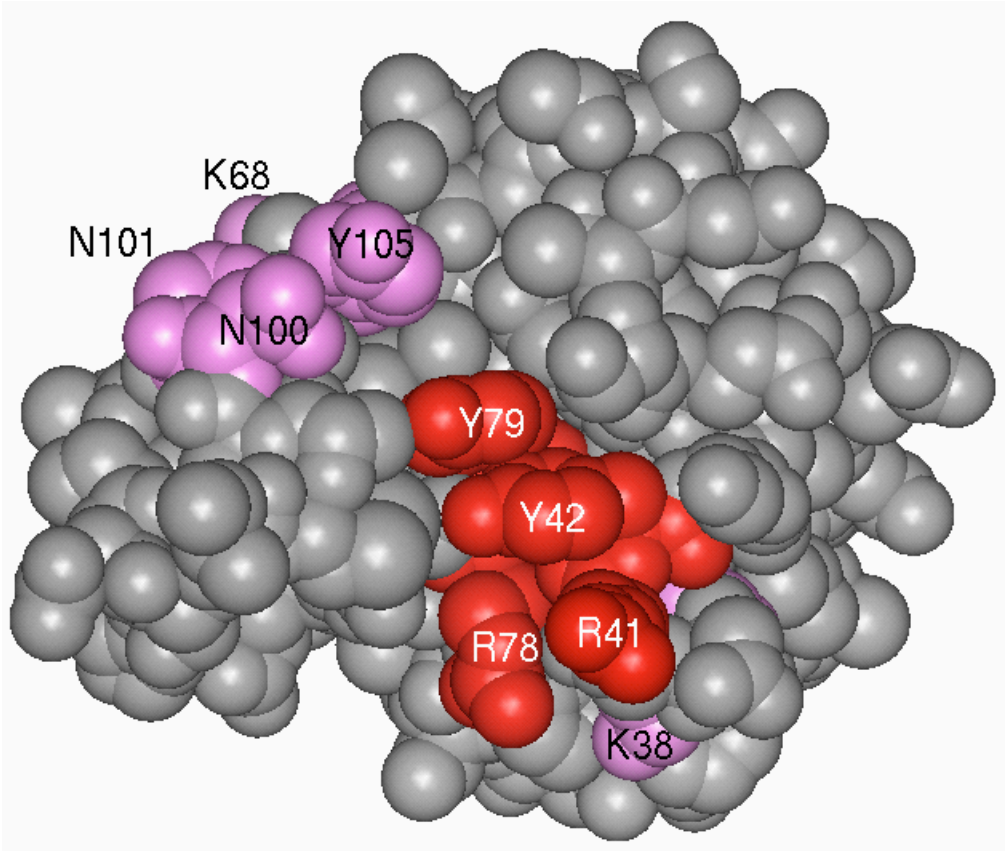

Figure 6a The hyaluronan binding site in CD44. *Residues which are, on the basis of mutagenesis, critical for ligand binding to CD44 are shown in red and residues which support binding are colored pink*

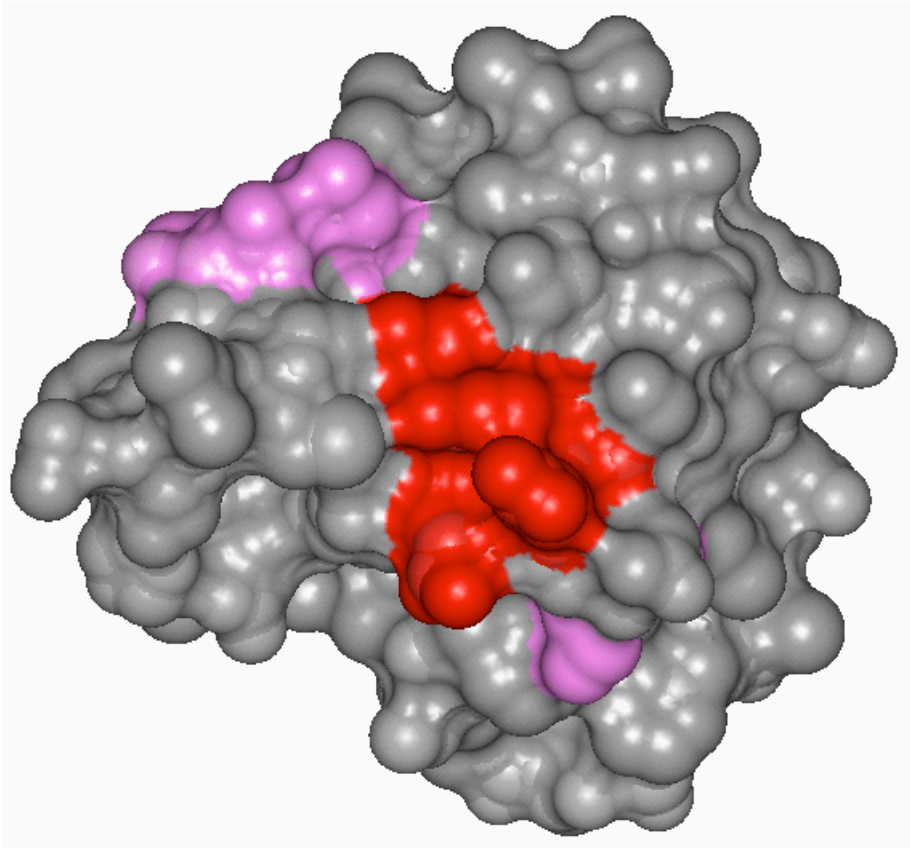

Figure 6b The hyaluronan binding site in CD44. *Solvent accessible surface of the model is rendered as a solid surface*

son of TSG-6 and ESL. TSG-6 resembles about half of the compact C-type lectin domain but does not include the calcium. The N-terminal segments of ESL and MBP share spurious sequence similarity with CD44 and other link modules [42]. Structure comparison shows that ~70 residues in TSG-6 can be superimposed on MBP with an rms deviation of close to 3 Å [18]. This means that it would have been very difficult to build molecular models of link modules, sufficiently accurate for structure-function studies, based on C-type lectins. By contrast, the link modules of CD44 and TSG-6 are ~35% identical in sequence. Taking conservative residue replacements into account, sequence similarity is at the 50% level [19], and this made more detailed modeling of CD44 possible.

CD44 molecular model and binding site analysis

Based on TSG-6, a molecular model of the HA binding domain in CD44 was generated using comparative modeling methods [19]. Figure 5 shows a superposition of the model and its parent structure. Ninety residues in CD44 superimposed on TSG-6 with a backbone rms deviation of ~1.5 Å. The model was used to guide mutagenesis experiments, identify residues important for HA binding, and outline HA binding site. In these studies, eight CD44 residues were identified which, when mutated, affected HA binding but not overall structural integrity of CD44, as assessed by binding of conformationally sensitive anti-CD44 monoclonal antibodies [19]. Figure 6a shows the location of these residues in the CD44 model. Four residues (R41, Y42, R78, Y79) are critical for the interaction with HA (i.e., mutation abolished binding) and form the center of the binding site, which is extended by other residues that contribute to binding (i.e., mutation reduced but did not abolish binding). In the model, critical residues and those which support binding form a coherent and extensive HA binding surface (Figure 6b), consistent with the finding that CD44 requires at least an HA hexasaccharide for effective binding [43].

Comparison of carbohydrate binding sites

The binding sites in MBP and ESL have been identified crystallograpically [23] and in conjunction with site-specific mutagenesis [24]. Carbohydrate binding to both MBP and ESL is strictly calcium-dependent, while CD44 does not require calcium for HA binding. Figure 7a shows a comparison of the carbohydrate binding sites in these molecules and illustrates that their locations approximately correspond. In addition, the dimensions of the binding sites correlate with the size of the ligands. MBP binds the smallest carbohydrate, a disaccharide, and the interactions are essentially limited to the calcium coordination sphere. In ESL, the conserved calcium is also involved in carbohydrate binding but the binding site is more extended, since a larger tetrasaccharide ligand is recognized. Figure 7b reveals a significant overlap of the binding sites in ESL and CD44, including the positions of some residues. For example, two tyrosines important for carbohydrate binding map to very similar positions. In the case of CD44, the size of the ligand further increases and, accordingly, the carbohydrate binding site is larger than in ESL. Since carbohydrate binding to CD44 is not supported by calcium coordination, a larger binding surface may be required to stabilize the interaction.

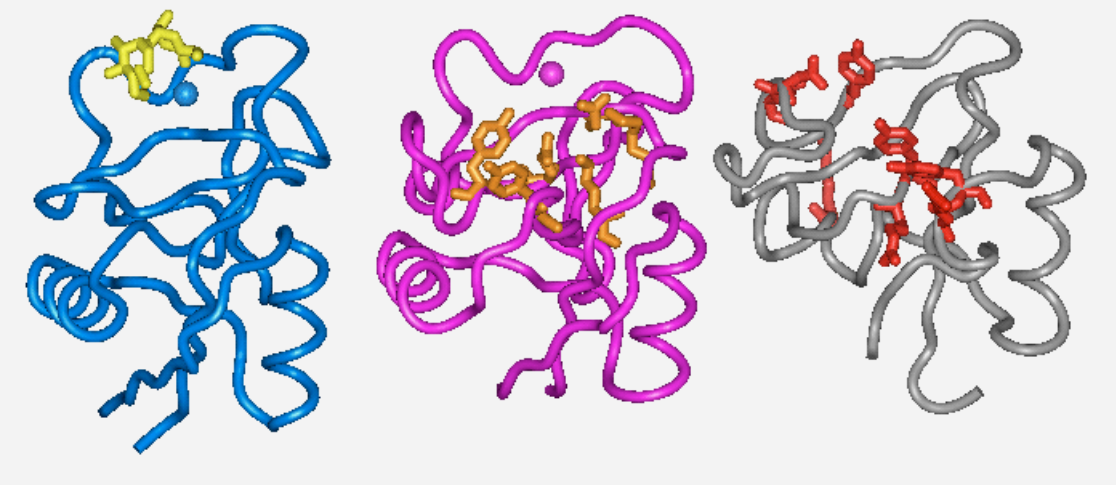

Figure 7a Comparison of carbohydrate binding sites in C-type lectins and CD44. *From the left to the right: Structure of MBP (blue) and ESL (magenta) and the CD44 molecular model (silver). The conserved calcium ions in MBP and E-selectin are depicted as spheres. MBP is shown in complex with dimannose (yellow), which directly binds to the calcium. Residues important for carbohydrate binding to ESL and CD44 are shown in gold and red, respectively*

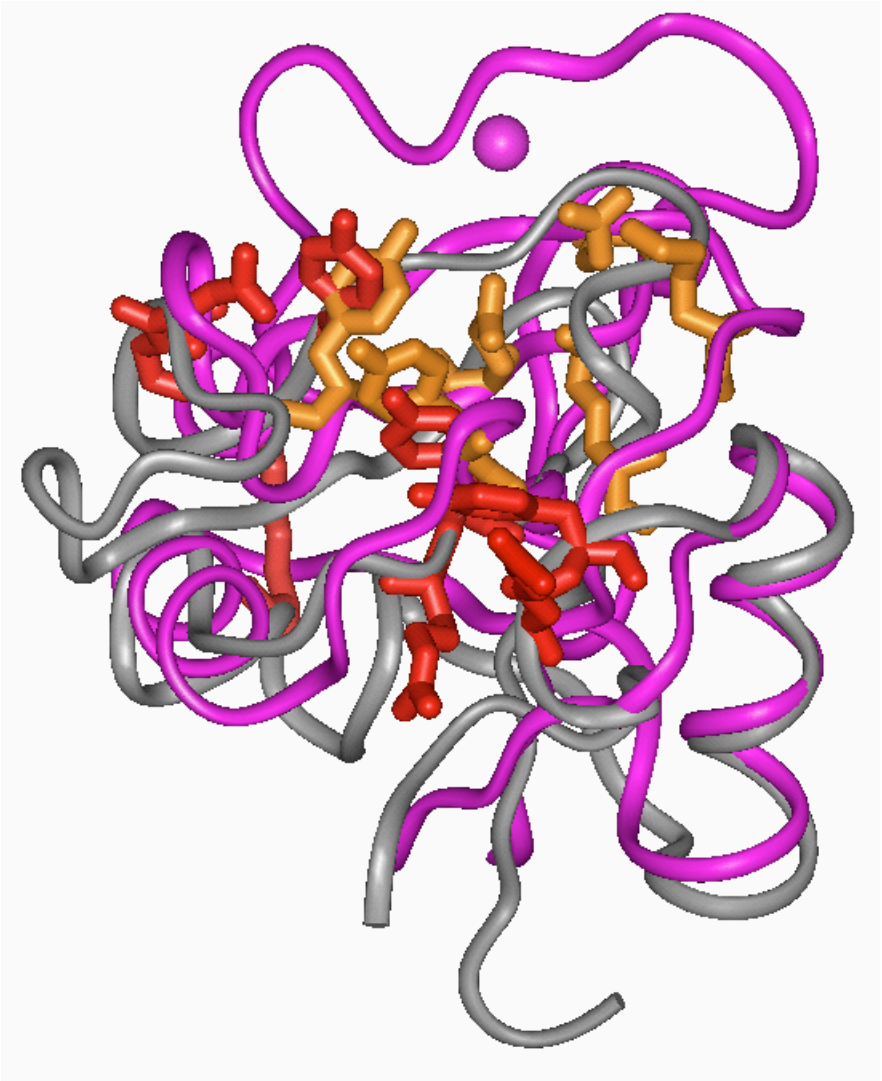

Figure 7b Comparison of carbohydrate binding sites in C-type lectins and CD44. *ESL and CD44 are superimposed and the binding sites are shown in a close-up view*

Evolutionary implications

MBP and ESL are structurally very similar but functionally distinct. Unlike the selectins, MBP is a serum protein, which binds mannose expressed on circulating pathogens and thereby triggers primitive immune responses [44]. In contrast, ESL and CD44, despite being structurally more diverse, are cell surface proteins and play similar roles in the adhesion of leukocytes. It follows that MBP may be an ancient protein, from which selectins have evolved to recognize more complex ligands and fulfill more specialized functions in the immune system. Furthermore, link modules, which are implicated in a variety of cellular functions [45], may have diverged later, as indicated by structural departures from the C-type lectin fold and differences in carbohydrate recognition. In conclusion, structure-function studies on C-type lectin domains and link modules provide some clues regarding the evolution of carbohydrate binding proteins with functions in the immune system.

Biological relevance of the molecular models

The studies on RANK and CD44 presented herein have made it possible to rationalize mutagenesis experiments and outline previously undescribed ligand binding sites. For RANK, the analysis of TNFRSF residue conservation in three dimensions led to the prediction of residues important for ligand binding. In the case of CD44, the model has made it possible to select residues for mutagenesis, map the carbohydrate binding site, and compare its location with other lectins. This has helped to better understand how diverse carbohydrate ligands are recognized by distantly related receptors. The identification and characterization of ligand binding sites in these cell surface proteins was dependent on the availability of sound molecular models and would not have been possible based on sequence analysis alone. The obtained results add to the knowledge of how specific receptor-ligand interactions are determined at the molecular level of detail.

Supplementary material Coordinates of the RANK molecular model have been deposited with the journal and are also available via e-mail from the author.

References

1. Smith, C. A.; Farrah, T.; Goodwin, R. G. *Cell* **1994**, *76*, 959.
2. Noelle, R. J.; Ledbetter, J. A.; Aruffo, A. *Immunol. Today* **1992**, *13*, 431.
3. Nagata, S.; Golstein, P. *Science* **1995**, *267*, 1449.
4. Mallet, S.; Barclay, A. N. *Immunol. Today* **1991**, *12*, 220.
5. Anderson, D. M.; Marashovsky, E.; Billingsley, W. L.; Dougall, W. C.; Tometsko, M. E.; Raoux, E. R.; Teepe, M. C.; DuBose, R. F.; Cosman, D.; Galibert, L. *Nature* **1997**, *390*, 175.
6. Banchereau, J.; Steinman, R. M. *Nature* **1998**, *392*, 245.
7. Banner, D. W.; D'Arcy, A.; Janes, W.; Gentz, R.; Schoenfeld, H.-J.; Broger, C.; Loetscher, H.; Lesslauer, W. *Cell* **1993**, *73*, 431.
8. Greer, J. *Proteins: Structure, Function, and Genetics* **1990**, *7*, 317.
9. Bajorath, J.; Stenkamp, R.; Aruffo, A. *Protein Science* **1993**, *2*, 1798.
10. Bajorath, J.; Aruffo, A. *Proteins: Structure, Function, and Genetics* **1997,** *27*, 59.
11. Bajorath, J.; Marken, J. S.; Chalupny, N. J.; Spoon, T. L.; Siadak, A. W.; Gordon, M.; Noelle, R. J.; Hollenbaugh, D.; Aruffo, A. *Biochemistry* **1995**, *34*, 9884.
12. Bajorath, J.; Aruffo, A. *J. Comp.-Aided Mol. Design* **1997**, *11*, 3.
13. Starling, G. C.; Bajorath, J.; Emswiler, J.; Ledbetter, J. A.; Aruffo, A.; Kiener, P. A. *J. Exp. Med.* **1997**, *185*, 1487.
14. Starling, G. C.; Kiener, P. A.; Aruffo, A.; Bajorath, J. *Biochemistry* **1998**, *37*, 3723.
15. Aruffo, A.; Stamenkovic, I.; Melnick, M.; Underhill, C. B.; Seed, B. *Cell* **1990**, *61*, 1303.
16. Knudson, C. B.; Knudson, W. *FASEB J*. **1993**, *7*, 1233.
17. Neame, P. J.; Barry, F. P. *Experientia* **1993**, *49*, 393.
18. Kohda, D.; Morton, C. J.; Parkar, A. A.; Hatanaka, H.; Inagaki, F. M.; Campbell, I. D.; Day, A. J. *Cell* **1996**, *86*, 767.
19. Bajorath, J.; Greenfield, B.; Munro, S. B.; Day, A. J.; Aruffo, A. *J. Biol. Chem.* **1998**, *273*, 338.
20. Drickamer, K. *J. Biol. Chem.* **1988**, *263*, 9557.
21. Springer, T. A. *Nature* **1990**, *346*, 425.
22. Lasky, L. A. *Science* **1992**, *258*, 964.
23. Weis, W. I.; Drickamer, K.; Hendrickson, W. A. *Nature* **1992**, *360*, 127.
24. Graves, B. J.; Crowther, R. L.; Chandran, C.; Rumberger, J. M.; Li, S.; Huang, K.-S.; Presky, D. H.; Familetti, P. C.; Wolitzky, B. A.; Burns, D. K. *Nature* **1994**, *367*, 532.
25. Bajorath, J. *J. Mol. Model.* **1998**, *4*, 1.
26. Ponder, J. W.; Richards, F. M. *J. Mol. Biol.* **1987**, *193*, 775.
27. Bajorath, J.; Aruffo, A. *J. Biol. Chem.* **1994**, *269*, 32457.
28. Weiner, P. K.; Kollman, P. A.; Nguyen, D. T.; Case, D. *J. Comput. Chem.* **1986**, *7*, 230.
29. Naismith, J. H.; Devine, T. Q.; Brandhuber, B. J.; Sprang, S. R. *J. Biol. Chem.* **1995**, *270*, 13303.
30. Murzin, A. G.; Bateman, A. *Proteins: Structure, Function, and Genetics* **1997**, *Suppl. 1*, 105.
31. Banchereau J.; Dubois B.; Fayette J.; Burdin N.; Briere F.; Miossec P.; Rissoan M. C.; van Kooten C.; Caux C. *Adv. Exp. Med. Biol.* **1995**, *378*, 79.
32. Naismith, J. H.; Sprang, S. R. *Trends. Biochem. Sci.* **1998**, *23*, 74.
33. Singh, J.; Garber, E.; Van Vlijmen, H.; Karpusas, M.; Hsu, Y.-M.; Zheng, Z.; Naismith, J. H.; Thomas, D. *Protein Sci.* **1998**, *7*, 1124.
34. Bajorath, J. *J. Mol. Model.* **1997**, *3*, 216.
35. Williams, A. F.; Barclay, A. N. *Ann. Rev. Immunol.* **1988**, *6*, 381.
36. Bork, P.; Holm, L.; Sander, C. *J. Mol. Biol.* **1994**, *242*, 309.
37. Bajorath, J.; Linsley, P. S. *J. Mol. Model.* **1997**, *3*, 117.
38. Bajorath, J.; Aruffo, A. *Protein Sci.* **1996**, *5*, 240.
39. DeGrendele, H. C.; Estess, P.; Picker, L. J.; Siegelman, M. H. *J. Exp. Med.* **1996**, *183*, 1119.
40. Arch, R.; Wirth, K.; Hofmann, M.; Ponta, H.; Matzku, S.; Herrlich, P.; Zoller, M. *Science* **1993**, *257*, 682.
41. Laurent, T. C.; Fraser, J. R. *FASEB J.* **1992**, *6*, 2397.
42. Brissett, N. C.; Perkins, S. J. *FEBS Lett.* **1996**, *388*, 211.
43. Underhill, C. B.; Chi-Rosso, G.; Toole, B. P. *J. Biol. Chem.* **1983**, *258*, 8086.
44. Drickamer, K.; Taylor, M. E. *Ann. Rev. Cell. Biol.* **1993**, *9*, 237.
45. Sherman, L.; Sleeman, J.; Herrlich, P.; Ponta, H. *Curr. Opin. Cell. Biol.* **1994**, *6*, 726.